

## Long-term performance of rubber bearing considering solar radiation effect

Paramashanti\*, Yasuo Kitane \*\*, Yoshito Itoh \*\*\*

\* M. of Eng., Dept. of Civil Eng., Nagoya University, Furo-cho, Chikusa-ku, Nagoya 464-8603

\*\* Ph.D., Assist. Prof., Dept. of Civil Eng., Nagoya University, Furo-cho, Chikusa-ku, Nagoya 464-8603

\*\*\* Dr. of Eng., Professor, Dept. of Civil Eng., Nagoya University, Furo-cho, Chikusa-ku, Nagoya 464-8603

The equivalent shear stiffness of a rubber bridge bearing increases over time due to the deterioration of rubber. It was assumed in the past aging estimation that rubber in the bearing and at the surface had the same temperature as its surrounding ambient temperature because rubber bearings were thought to be usually in the shadow as they are installed between the superstructure and the substructure. However, in the actual environment, there are many bearings that are exposed to solar radiation that causes bearing temperature to increase. To evaluate the effect of solar radiation on the bearing temperature, bearing surface temperatures were measured for a bearing installed on an elevated highway in Nagoya, Japan. In addition, to understand a temperature variation in a bearing, a bearing model was manufactured, and a temperature measurement of internal temperature was carried out. Long-term performance of rubber bearing by considering solar radiation effect on bearing temperature was investigated.

*Keywords: rubber bearing, base isolation, deterioration, temperature, solar radiation*

### 1. INTRODUCTION

Rubber has a long history of applications in bridge bearings due to its special properties such as high elasticity and large elongation at failure. Although the application of rubber bearings began more than 100 years ago<sup>1)</sup>, the number of applications has increased dramatically in recent decades, especially after the Hyogo-ken Nambu earthquake in Japan. Rubber bearings are now used worldwide as one of the standard methods of supporting superstructure<sup>2)</sup>.

It is well known that the properties of rubber change over time due to aging, eventually to the point where the material is no longer capable of satisfying its function. Watanabe et al.<sup>3)</sup> reported that the shear stiffness of the forty-year old natural rubber (NR) bearings increased by about 10%, which were installed in the Pelham Bridge in England, where the yearly average temperature is 9.2°C.

A series of accelerated exposure tests were performed by Itoh et al.<sup>4), 5), 6), 7)</sup> on various rubber materials to investigate the degradation effects of different environmental factors. It was found that the thermal oxidation is the most predominant degradation factor affecting the rubber material of bridge bearings. Matsuda et al.<sup>8)</sup> examined the deterioration

characteristics of bridge rubber bearings during their lifespan by recalling some bearings in use and performing the mechanical tests for those bearings. Itoh et al.<sup>9)</sup> investigated the effect of ultraviolet irradiation on four kinds of rubber materials typically used for bridge bearing through accelerated aging test. It was found that ultraviolet irradiation only affects the mechanical properties of the rubber near the surface, which receives the sunlight directly. Since bearing has surface rubber of a certain thickness, the effect of ultraviolet irradiation cannot progress into the inner rubber, and will not influence the general performance of the bridge rubber bearing. Although the aging was proved to cause the properties of rubber to change, the behaviors of deteriorated bridge rubber bearings during their lifespan are not considered in the current design specifications<sup>10)</sup>.

Since heat oxidation is one of the major deterioration factors for rubber, temperature has a significant influence on the deterioration process of rubber. The equivalent shear stiffness of a bridge rubber bearing increases over time due to the deterioration of rubber, and the higher the rubber temperature, the faster it increases. Itoh et al.<sup>5)</sup> proposed formulas to estimate the increase in the equivalent stiffness due to aging. For the bearing size of 400 mm x 400 mm, the increase in the equivalent shear stiffness of an NR bearing in Naha where the yearly average

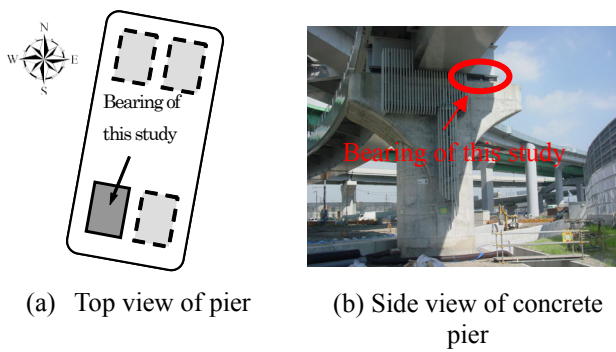


**Fig. 1** Bearing location and orientation

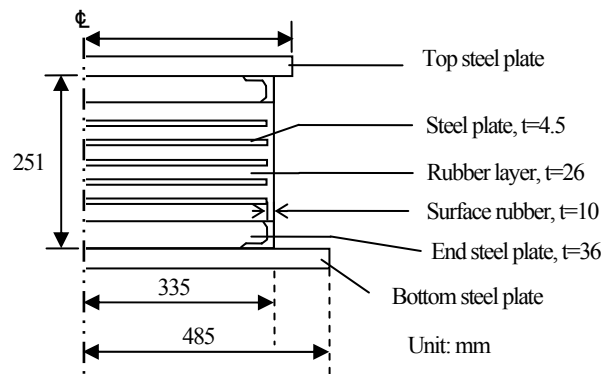


**Fig. 2** Bearing dimensions

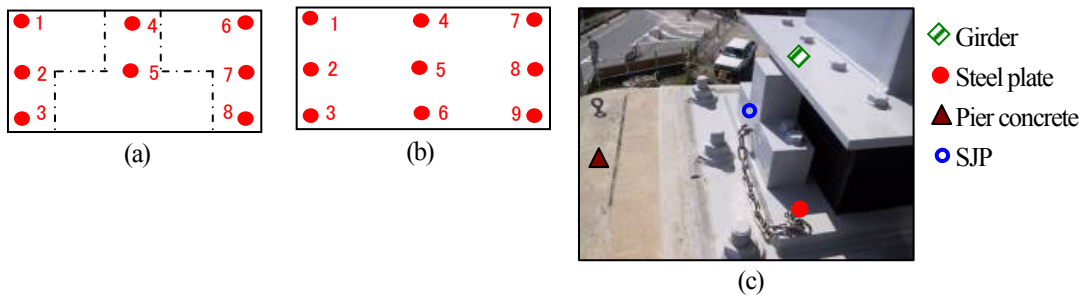


**Fig. 3** Measurement locations: (a) south and north bearing surfaces, (b) west and east bearing surfaces, and (c) other measurement objects

ambient temperature is  $22.7^{\circ}\text{C}$  reaches 26% of the initial stiffness, while in Sapporo with the average temperature of  $8.5^{\circ}\text{C}$ , the increase is about 15%.

Itoh et al.<sup>5)</sup> proposed to use the yearly average ambient temperature to predict aging of rubber bearings. It is assumed that rubber in the bearing has the same temperature as its surrounding ambient temperature because rubber bearings are thought to be usually in the shadow as they are installed between superstructure and substructure. However, in the actual environment, there are many bearings that are exposed to solar radiation that causes bearing temperature to increase. To evaluate the effect of solar radiation on the bearing temperature, bearing surface temperatures were measured in this study on a bearing installed in an elevated highway in Nagoya, Japan, in summer and winter seasons.

To accurately evaluate the long-term performance of rubber bearings that are exposed to solar radiation during the day, it is necessary to obtain the information on temperature variation inside a bearing. In this study, an internal temperature measurement was also performed on a bearing model.

The objectives of this study are to (1) evaluate the effect of solar radiation on the bearing surface temperature, (2) evaluate the effect of solar radiation on the internal bearing temperature, and (3) investigate the long-term performance of rubber bearing by considering solar radiation effect on bearing temperature.

## 2. TEMPERATURE MEASUREMENT ON BEARING INSTALLED IN THE BRIDGE

### 2.1 Bearing for the Measurement

The bearing is a high damping rubber (HDR) bearing of 670 mm x 670 mm installed on a concrete pier. The orientation of the bearing on the pier is shown in Fig. 1. As shown in Fig. 1, the bearing surfaces of the south and west sides can receive sunlight much more than the north and east sides. As shown in Fig. 2, the bearing has six rubber layers with a thickness of 26 mm, five layers of inner steel plates with a thickness of 4.5 mm, and two 36 mm thick steel end plates. The bearing is covered with NR with a thickness of 10 mm. Steel blocks to control bearing displacement in the transverse direction of the bridge are installed in front of the south and north surfaces, which are referred to as steel joint protections.

### 2.2 Measurement Program

The measurement in the summer season was taken from August 25 to September 2, 2007, while in winter it was from January 18 to January 25, 2008. Bearing temperatures were measured by using T-type thermocouples with a wire diameter of 0.32 mm, at nine points on the west and east sides and eight points on the north and south sides. Temperatures of steel girder, bottom and top steel plates, a steel joint protection (SJP), and the top surface of the concrete pier were also measured on

Table 1 Meteorological conditions for the summer measurement of bearing installed in the bridge

Date	Weather condition		Average wind velocity (m/s)	Ambient temperature (°C)			Precipitation (mm)	Sunshine duration (h)
	06:00 - 18:00	18:00 - 06:00		Average	Max	Min		
07/8/25	Slightly cloudy after the clear	Clear after the slightly cloudy	2.1	29.8	35.7	25.1	--	10.6
07/8/26	Slightly cloudy after the clear	Slightly cloudy	2.2	29.2	36.1	23.6	--	11.9
07/8/27	Slightly cloudy	Slightly cloudy	2.3	30.4	35.8	25.1	--	11.0
07/8/28	Cloudy	Clouding temporarily clear	2.5	28.4	31.2	26.4	0	1.7
07/8/29	The clouding occasionally rain, the thunder is accompanied	Cloudy after the clear	1.8	26.5	30.6	24.1	5	1.8
07/8/30	The clouding occasionally rain, the thunder is accompanied	The clouding occasionally rain, the thunder is accompanied	2.3	26.1	29.8	24.2	0	--
07/8/31	The clouding occasionally rain, the thunder is accompanied	Clear temporarily the clouding	2.9	25.5	29.9	23.4	3.5	0.6
07/9/1	Clear	The clouding temporarily the rain	2.9	26.1	31.8	21.8	0	7.6
07/9/2	The clouding temporarily the rain	The clouding temporarily the rain	1.8	24.3	26.3	21.4	1	--

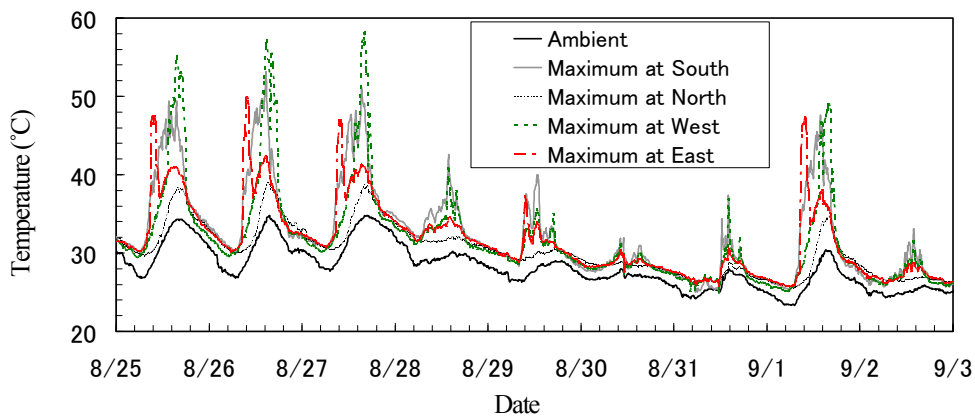


Fig. 4 Ambient temperature and bearing surface temperature in the summer measurement

each side of the bearing. The measurement positions are shown in Fig. 3. In addition, solar radiations were measured on the south and north sides using pyranometers with sensitivity of 7 mV/kW/m<sup>2</sup> for wave lengths of 305-2800 nm. Ambient temperature was also measured by thermocouple.

### 2.3 Measurement Results

Weather conditions, provided by Japan Meteorological Agency (JMA), during the summer measurement period are shown in Table 1. The duration of sunshine is very short on August 30-31 and September 2 due to rain. Fig. 4 compares ambient and bearing surface temperatures in the summer measurement, and Fig. 5 shows solar radiations for the

corresponding period.

During the summer measurement period, the maximum, minimum, and average ambient temperatures were 35°C, 23°C, and 28°C, respectively, while in the winter measurement, they were 0°C, 0°C, and 5°C, respectively. By examining Figs. 4 and 5, it is apparent that bearing surface temperature is influenced by solar radiation. The east surface receives solar radiation in the morning, the south side does during the day, the east side does in the late afternoon, and surface temperature changes accordingly. In the summer measurement, the maximum bearing temperature was 58°C, which was 23°C higher than the ambient temperature at the same time. A larger difference was found in the winter measurement as the maximum bearing surface temperature was

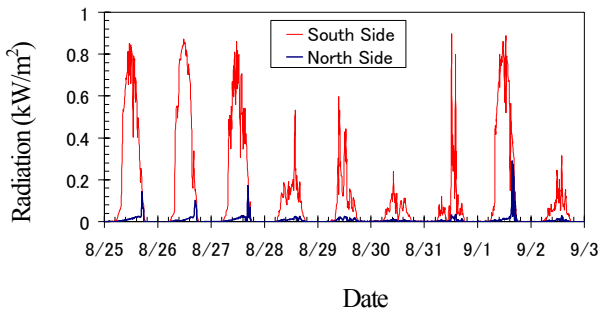


Fig. 5 Solar radiation in summer season

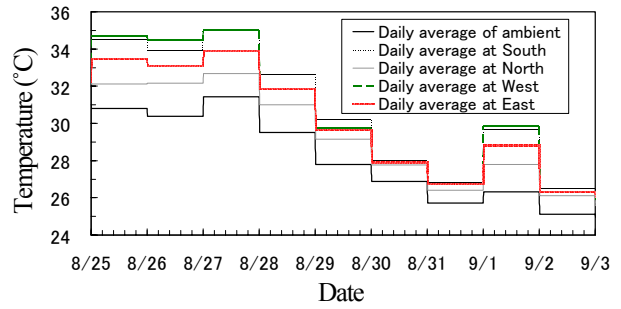


Fig. 6 Daily average temperatures in the summer measurement

46°C, which was 36°C higher than the ambient temperature. The maximum bearing temperature occurred on the west side and the south side in the summer and winter measurements, respectively.

The results from the field measurements show that the difference between the surface temperature and the ambient temperature becomes significantly large when the surface receives direct solar radiation on a sunny day, and the maximum difference can be more than 20°C. However, on the bearing surface in the shadow, the surface temperature tends to be close to the ambient temperature as solar radiation is small, and the maximum difference is only about 2°C.

The daily average temperatures of the summer measurement are shown in Fig. 6. It can be seen that the difference between the daily average bearing surface temperature and the ambient temperature is larger on sunny days, which is about 4-6°C, while on rainy days it is about 1-2°C. The differences seem to be slightly greater in the winter measurement than the summer.

The difference between daily average values of surface temperature and ambient temperature is much smaller than the difference between the maximum values of bearing and ambient temperatures, implying that the bearing surface does not keep the heat energy from solar radiation, but loses the heat soon after it receives. It should also be noted that the surface temperature of the north side that is in the shadow tends to be very close to the ambient temperature even when other surfaces have very high temperatures due to solar radiation, which implies that solar radiation on one surface does not affect temperatures of other surfaces significantly.

Temperatures of the surrounding areas were measured to understand boundary conditions of the bearing. The results show similar variations to those of bearing surface temperatures, and their temperatures differ significantly from the ambient temperature only when they are exposed to solar radiation. The difference between average temperatures over measurement period and average ambient temperature ranged from 1°C to 3°C for the east, south, and west sides in summer, while the difference ranged from 1°C to 2°C for those sides in winter. On the north side, temperatures of surrounding areas were very close to the ambient temperature.

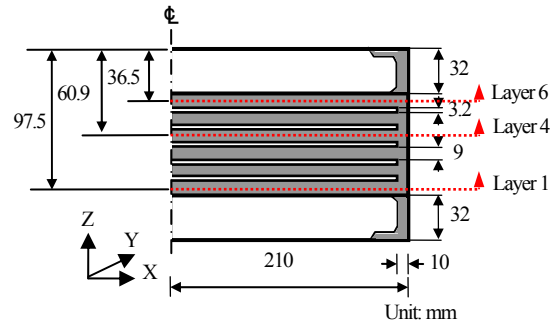


Fig. 7 Bearing model for the internal temperature

### 3. INTERNAL BEARING TEMPERATURE MEASUREMENT

#### 3.1 Specimen

To understand a temperature variation inside a rubber bearing, surface and internal temperatures of a bearing model were measured. The size of bearing is 420 mm x 420 mm x 134 mm as shown in Fig. 7. The bearing is an HDR bearing, and has six rubber layers with a thickness of 9 mm, end steel plates with a thickness of 32 mm, five inner steel plates with a thickness of 3.2 mm, and surface rubber with a thickness of 10 mm. The bearing has vertical holes for thermocouples reaching the three different rubber layers, and their depths are 37 mm, 61 mm, and 98 mm as shown in Fig. 7, which are at Layers 1, 4, and 6, referred to as to the bottom, middle, and top layers of bearing. There are totally 36 measurement points: 9 points in either at Layer 1 or 6, and 18 points in Layer 4. Temperature measurement positions and the numbering system used in the measurement are shown in Fig. 8. To measure bearing's internal temperature, sheathed thermocouples were used so that thermocouples could easily reach the desired locations inside the bearing. Measurement data were recorded every 10 minutes.

#### 3.2 Internal Temperature Response to Step Temperature

In order to estimate a convective coefficient of bearing surface rubber, the response of internal temperature to stepwise temperature changes of ambient temperature was measured in the

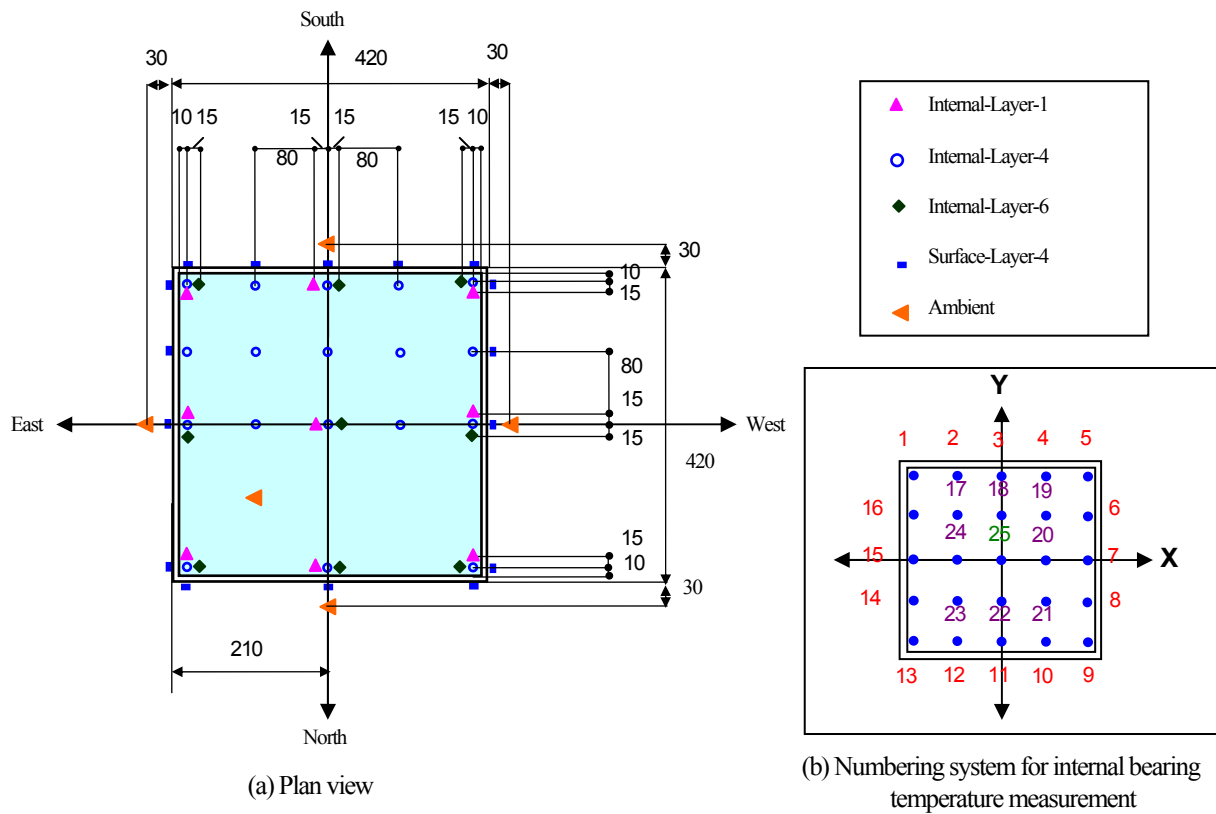


**Fig. 8** Measurement positions and numbering system for internal measurement

temperature-controlled room with a size of 3.6 m x 2.25 m at Tokai Rubber Industries, Ltd. The convective coefficient will be used for the analytical model of rubber bearing in heat transfer analysis. The ambient temperature was controlled by using an air conditioner. The measurement was carried out for 7 days. The temperature setting of the air conditioner was changed every 24 hours between a low temperature of 17°C and a high temperature of 30°C. In this measurement, internal bearing temperatures were only measured in a quarter part of the bearing. Referring to the numbering system shown in Fig. 8, internal temperatures were measured at Pts. 1, 2, 3, 15, 16, 17, 18, 24, and 25 at Layer 4, and Pts. 1, 3, 15, and 24 at Layers 1 and 6. Ambient temperature was measured at four locations around the bearing.

The time histories of ambient and internal bearing temperatures at Layer 4 are shown in Fig. 9. The ambient temperature shown in Fig. 9 is the average of the four locations. As it can be seen in Fig. 9, the ambient temperature reached the stable temperature within 1-1.5 hours after the temperature setting was changed. In Fig. 9, L4-25 means the internal temperature at Pt. 25 at Layer 4. Internal bearing temperature changes gradually due to the change of ambient temperature, and it could not fully reach the ambient temperature within 24 hours after a step temperature change. Temperatures at all points in the bearing show the similar value to each other. The largest

difference among points occurs when the ambient temperature changes from low to high or high to low temperatures, which is about 0.6°C.

### 3.3 Measurement for Bearing Exposed to Solar Radiation

To understand a temperature variation in the bearing exposed to solar radiation, surface and internal temperatures of the bearing model were measured. The measurement was carried out on the roof of a four-story building in Nagoya University, Japan. The wooden box was used to change conditions of solar radiation. The box has louvered walls and openings between walls and its

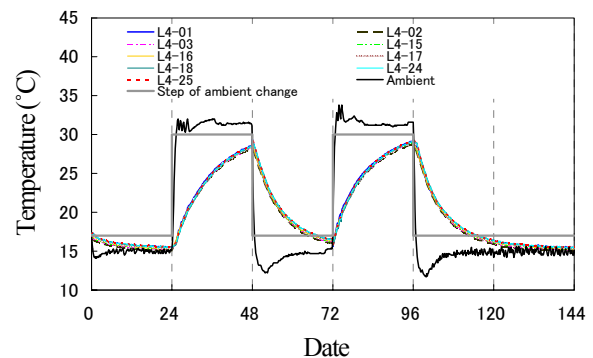


**Fig. 9** Step of ambient temperature change and internal bearing temperatures in Layer-4

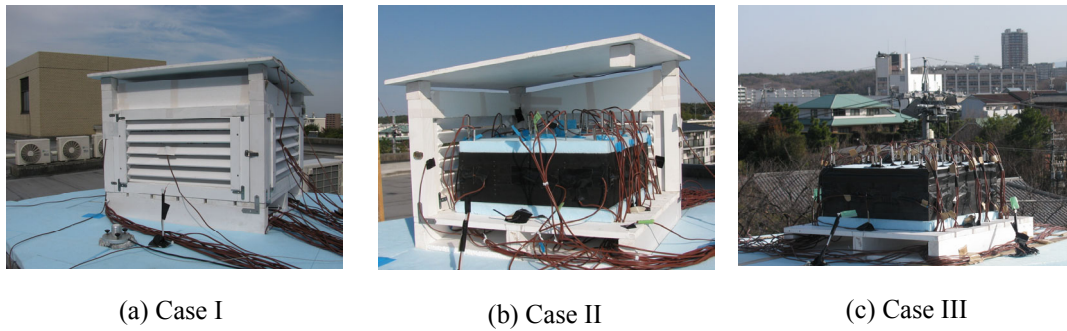
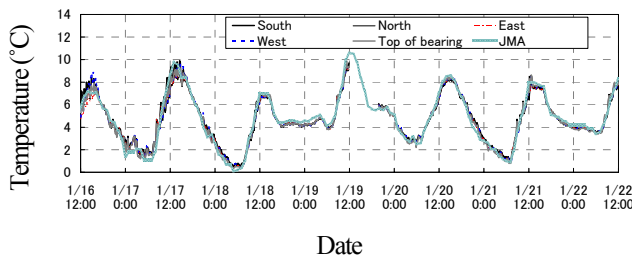
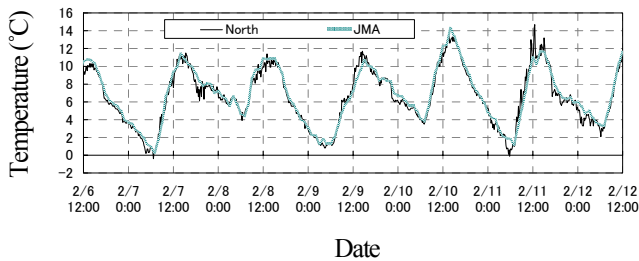


Fig. 10 Measurement condition

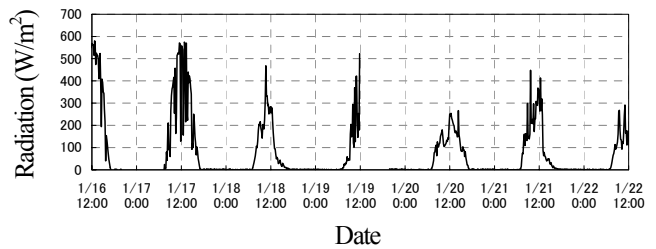


(a) Case I measurement

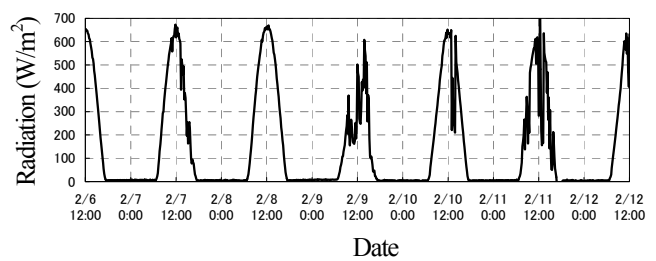


(b) Case III measurement

Fig. 11 Ambient temperature



(a) Case I measurement



(b) Case III measurement

Fig. 12 Solar radiation

roof so that air in the box can circulate well. The box size is 600 mm x 600 mm. The height of the box roof is 530 mm on the front side, and the roof has an inclination of about 5° to allow the rain water to flow down. Walls of the box can be removed so that the conditions on how bearing receives solar radiation can be changed.

In this study, three cases were examined in the measurement: (1) the bearing was fully in the shadow, (2) two vertical sides of the bearing were exposed to solar radiation, and (3) the bearing was fully exposed to solar radiation. Fig. 10 shows the measurement conditions for all cases.

Surface bearing temperature was measured on all sides by using standard T-type thermocouples at the same height as Layer 4 of internal measurement points. There were five points of surface measurement positions on the south side, four points on the west and east sides, and three points on the west side. Ambient temperature was also measured at five points inside the

box by using standard T-type thermocouples. Those five points were in front of all bearing surfaces and over the top of bearing. In addition, solar radiation was measured on the south side using a pyranometer with sensitivity of 7 mV/kW/m<sup>2</sup> for wave lengths of 305-2800 nm.

Measurements were taken from January 16 to 22, 2009, for Case I, from January 26 to February 2, 2009, for Case II, and from on February 6 to 12, 2009, for Case III.

### 3.4 Measurement Results

Measurement results for Case I and Case III are shown in Fig. 11 to Fig. 16. Weather conditions and other meteorological data during the measurement period are shown in Table 2. In Case I the data recording was stopped for a period from 12:00 to 19:40 of January 19 to check the measurement device. Ambient temperature and solar radiation data from the measurement are shown in Figs. 11 and 12. For the results summary, the average



Table 2 Meteorological conditions during the bearing internal temperature measurement

(a) Case I

Date	Weather condition of Case III		Average wind velocity (m/s)	Ambient temperature (°C)			Precipitation (mm)	Sunshine duration (h)
	06:00 - 18:00	18:00 - 06:00		Average	Max	Min		
09/1/16	Sunny	Temporarily cloudy after sunny	1.7	3.0	8.5	-2.0	--	8.7
09/1/17	Sunny	Sunny	2.1	4.7	10.5	0.5	0.0	7.3
09/1/18	Rainy after cloudy	Temporarily cloudy after rainy	1.6	3.6	7.9	0.0	9.5	0.5
09/1/19	Sunny occasionally cloudy, accompanied by rain	Slightly cloudy after sunny	3.9	6.4	11.5	4.0	4.5	3.9
09/1/20	Cloudy temporarily rain	Slightly cloudy after sunny	2.1	5.0	9.0	2.0	--	0.0
09/1/21	Temporarily rain after cloudy	Cloudy after rainy	1.6	4.4	8.8	0.4	8.0	0.8
09/1/22	Rainy after cloudy	Rainy	1.4	6.3	8.7	3.3	7.5	0.4

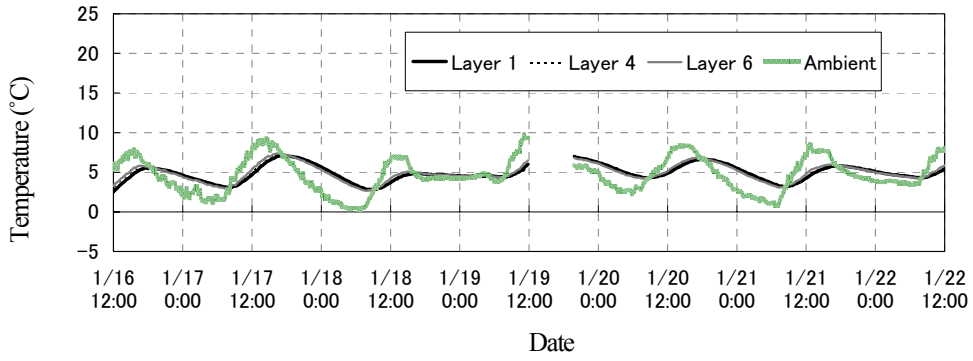
(b) Case III

Date	Weather condition of Case III		Average wind velocity (m/s)	Ambient temperature (°C)			Precipitation (mm)	Sunshine duration (h)
	06:00 - 18:00	18:00 - 06:00		Average	Max	Min		
09/2/6	Perfectly sunny	Temporarily slightly cloudy after sunny	5.6	7.2	11.5	3.7	--	10.0
09/2/7	Slightly cloudy after sunny	Sunny occasionally cloudy	2.0	6.3	11.8	0.2	--	8.8
09/2/8	Sunny	Temporarily slightly cloudy after sunny	4.5	7.2	11.8	3.1	--	9.8
09/2/9	Cloudy	Cloudy occasionally sunny	1.9	6.2	11.5	0.9	0.0	1.8
09/2/10	Sunny	Sunny	4.0	8.2	14.6	3.8	0.5	9.6
09/2/11	Sunny occasionally cloudy temporarily rainy	Sunny after rainy	2.2	6.4	12.6	0.9	2.5	5.8
09/2/12	Slightly cloudy after sunny	Temporarily sunny after cloudy	2.4	7.9	13.5	3.2	--	7.0

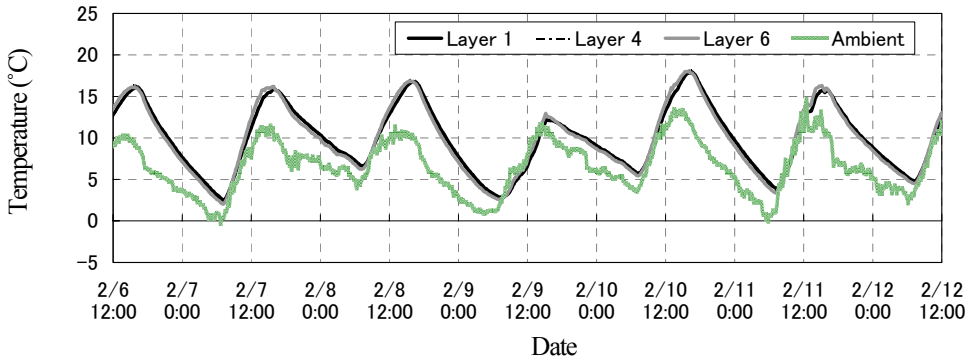
of ambient temperature data from five points were used for Case I measurement. However, to avoid the measurement positions that receive solar radiation, Case II only used the average of the north and the east sides, and Case III used the result from the north side. In Fig. 11, JMA means the data provided by Japan Meteorological Agency. As it can be seen in Fig. 11, the measured ambient temperature is close to the JMA data.

The internal bearing temperatures are shown in Fig. 13. Fig. 13 shows the average temperature over measurement points of each layer and the ambient temperature. Average bearing internal temperatures of all three layers are close to each other.

The maximum difference between the internal and ambient temperatures are about 4°C and 7°C for Case I and Case III, respectively. Average bearing internal temperature of Case I is higher than average ambient temperature from the evening to the early morning, and it becomes lower from the morning to the afternoon. In Case III, the internal temperature is close to the ambient temperature from the morning to the time before noon. Beyond that time, the internal temperature is higher than the ambient temperature. From Fig. 14, it can be seen that when the bearing is fully in the shadow, the daily average of bearing internal temperature is very close to the ambient temperature, regardless of weather conditions.

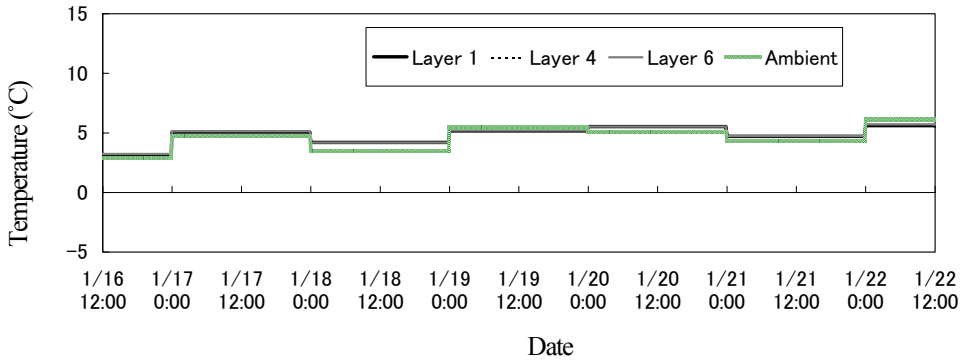


(a) Case I measurement

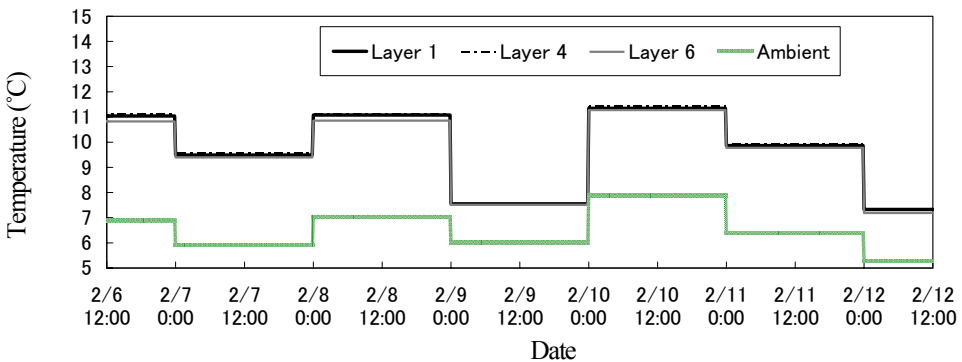


(b) Case III measurement

**Fig. 13** Average of internal temperature



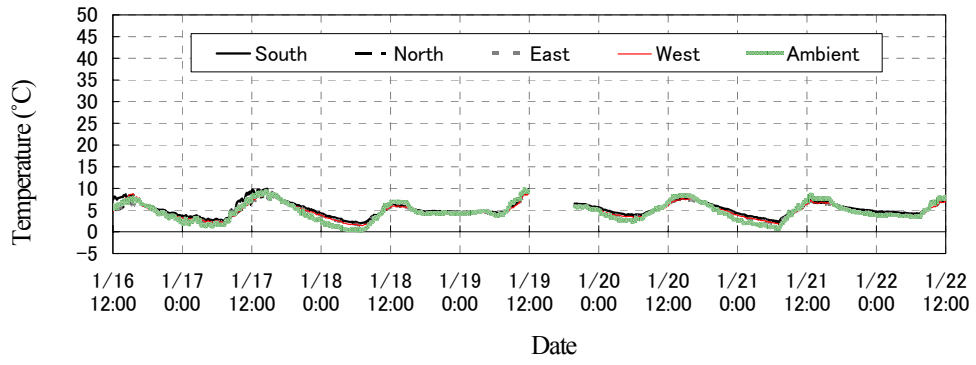
(a) Case I measurement



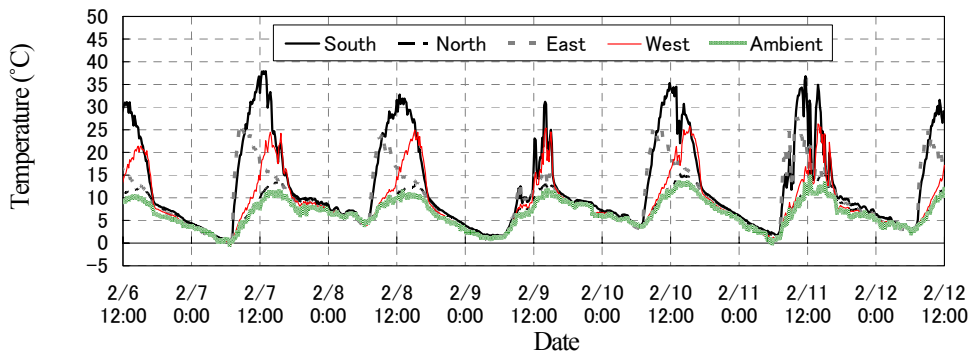
(b) Case III measurement

**Fig. 14** Daily average of internal and ambient temperatures



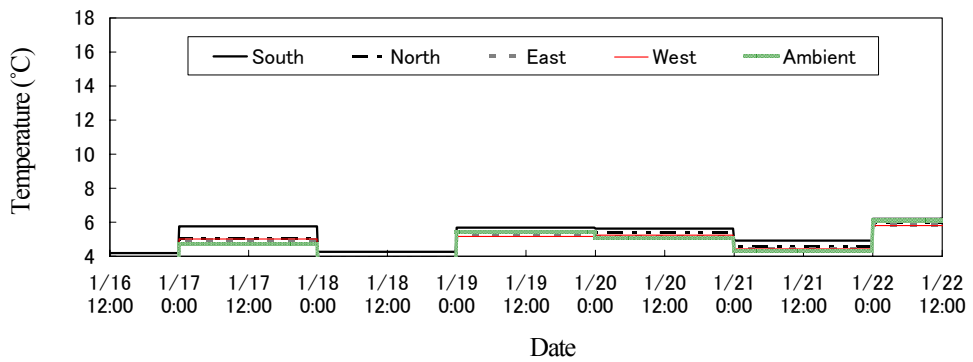


(a) Case I measurement

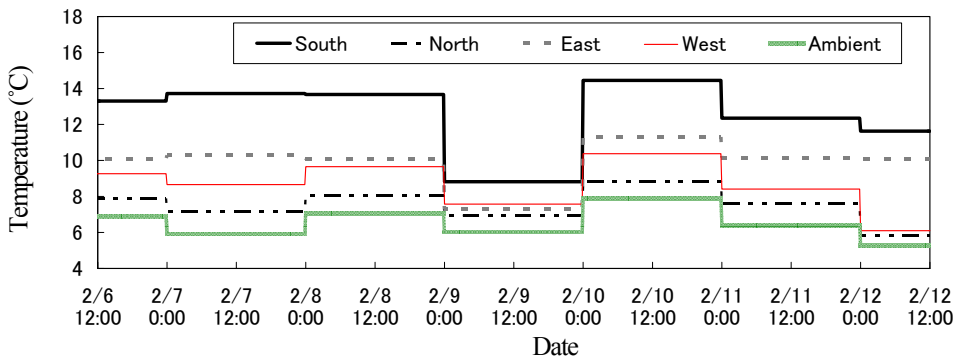


(b) Case III measurement

**Fig. 15** Average of surface temperature



(a) Case I measurement



(b) Case III measurement

**Fig. 16** Daily average of surface and ambient temperatures

However, when bearing is exposed to solar radiation, the difference between the daily average of internal bearing and ambient temperature is about 2-7°C, and it depends on the weather condition. The larger difference is found on a sunny day. The difference between time average values of the internal bearing and ambient temperatures over the measurement period is about 3°C in Case III.

Surface bearing temperatures are shown in Fig. 15. The value in the figure is the average of all measurement points on each side. When the bearing is fully in the shadow, the surface bearing temperature is close to the ambient temperature, while when the bearing surface is exposed to solar radiation, the surface bearing temperature shows a higher value than the ambient temperature. It can be seen that for Case III the maximum difference is about 30°C on the south side. The north surface exhibits temperatures close to the ambient. As shown in Fig. 16, the maximum difference between daily average values of the surface and ambient temperatures for Case I is less than 1°C. However, in Case III, the difference between daily average values of the surface and ambient temperatures is about 1-8°C. The difference between surface bearing and ambient temperatures for time average during the measurement period is about 3°C.

Temperature variations in Layer 4 on the center lines along E-W and N-S directions of Case III on a sunny day of February 10, 2009 are shown in Figs. 17 and 18, respectively. Five different time instances are examined: (1) ambient temperature becomes the maximum, (2) ambient temperature becomes the minimum, (3) the center of bearing (L4-25) becomes the maximum temperature, (4) L4-25 becomes the minimum temperature, and (5) the surface bearing temperature becomes the maximum. As it can be seen in Figs. 17 and 18, solar radiation affects the temperature variation inside the rubber bearing. The large temperature variation inside the bearing occurs within about 20 mm from the bearing surface. Temperature is almost uniform beyond that depth, and the variation is only about 2-3°C. The largest variation in the 20 mm region occurs when the surface reaches the maximum temperature as an effect of solar radiation, where there is a difference of 25°C between the surface and the depth of 20 mm. As the bearing has 10 mm thick NR surface rubber, shown as the grey zone in Figs. 17 and 18, there is about 10 mm of internal rubber thickness that experiences a large temperature increase as a result of solar radiation.

#### 4. LONG-TERM PERFORMANCE OF RUBBER BEARING CONSIDERING SOLAR RADIATION

##### 4.1 Bearing Temperature Prediction

To investigate the effect of solar radiation on long-term performance of rubber bearing, bearing temperature has to be predicted. In this study, the internal of bearing temperature is estimated based on the measurement results. As it can be

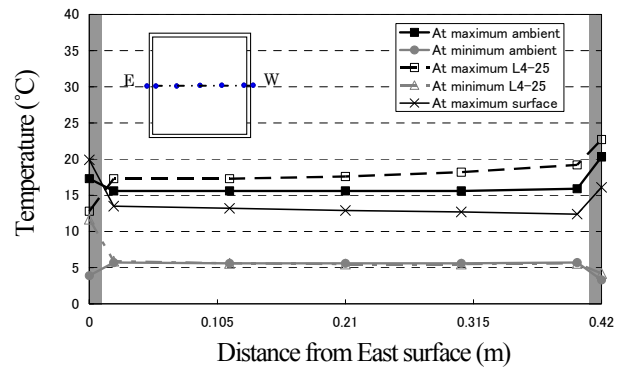


Fig. 17 Internal bearing temperature variation along the E-W centerline in Layer 4 for Case III

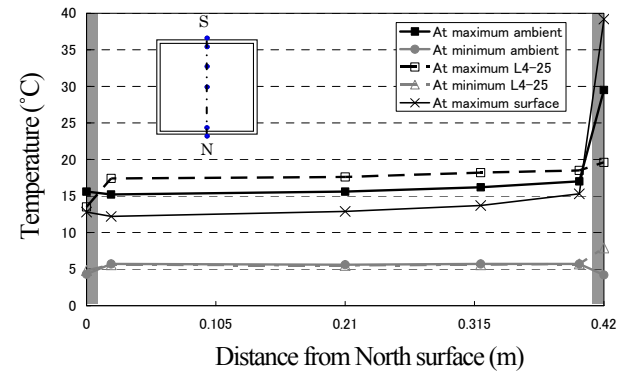


Fig. 18 Internal bearing temperature variation along the N-S centerline in Layer 4 for Case III

concluded from Fig. 14, the difference in daily average temperatures between the internal bearing and ambient is affected by the solar radiation of the day. By comparing the daily averages of the ambient and internal bearing temperatures, the relationship between the temperature difference and a daily solar radiation is examined as shown in Fig. 19. The daily temperature difference of each layer and daily solar radiation shown in Fig. 19 are calculated by using the following equations:

$$T_i^{int} = \frac{1}{m} \sum_{j=1}^m T_{ji}^{int} \quad (1)$$

$$T_{AvgInt} = \frac{1}{n} \sum_{i=1}^n T_i^{int} \quad (2)$$

$$T_i^{amb} = \frac{1}{p} \sum_{k=1}^p T_{ki}^{amb} \quad (3)$$

$$T_{AvgAmb} = \frac{1}{n} \sum_{i=1}^n T_i^{amb} \quad (4)$$

$$\Delta T = T_{AvgInt} - T_{AvgAmb} \quad (5)$$

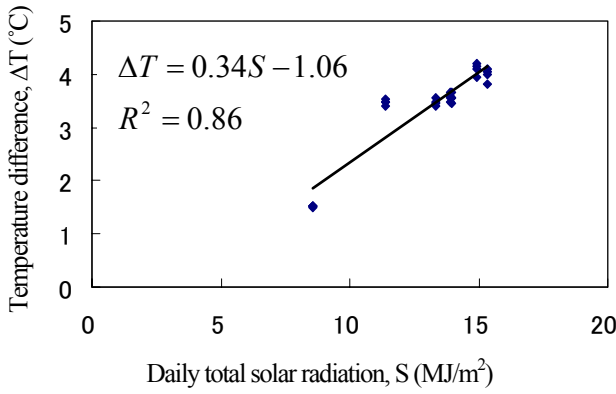


**Fig. 19** Relationship between daily total solar radiation and daily difference of internal bearing and ambient temperatures

$$S = \sum_{i=1}^n (S_i + S_{i+1}) \frac{\Delta t}{2} \quad (6)$$

where  $\Delta T$  is the temperature difference between daily average internal bearing and ambient temperatures,  $T_{AvgInt}$  is the daily average internal bearing temperature,  $T_{AvgAmb}$  is the daily average ambient temperature,  $T_{ji}^{int}$  is the internal bearing temperature data of the  $j$ -th measurement point at the  $i$ -th data in the day,  $T_i^{int}$  is the average internal bearing temperature of the horizontal cross section of bearing at the  $i$ -th data in the day,  $T_{ki}^{amb}$  is the ambient temperature data of the  $k$ -th measurement position at the  $i$ -th data in the day,  $T_i^{amb}$  is the average ambient temperature of  $p$  measurement positions at the  $i$ -th data in the day,  $S_i$  is the  $i$ -th solar radiation data,  $S$  is the daily total solar radiation,  $\Delta t$  is the time interval of measurement, which is 10 minutes,  $m$  is the number of internal bearing temperature measurement points,  $p$  is the number of ambient temperature measurement positions, and  $n$  is the number of data in a day.

By assuming that internal bearing temperature is uniform in the horizontal cross section of a bearing, the heat used to increase bearing temperature from solar radiation can be calculated by the following equation:

$$\Delta Q = c\rho V\Delta T = c\rho V(T_2 - T_1) \quad (7)$$

$\Delta Q$  represents the difference between heat from solar radiation and heat lost by the bearing through convection and radiation,  $c$  is specific heat,  $\rho$  is the density,  $V$  is the bearing volume, and  $\Delta T$  is the temperatures difference before and after the bearing receiving solar radiation.  $T_2$  is temperature after bearing receiving solar radiation and  $T_1$  is temperature before receiving solar radiation, which is equal to the ambient temperature. From Eq. (7), it can be seen that  $\Delta Q$  has a linear relationship with the temperature difference. In this study, by assuming  $S \propto \Delta Q$ , a relationship between solar radiation and the temperature difference can be estimated. From Fig. 19 the regression relationship to estimate the temperature difference  $\Delta T$  between internal bearing and

ambient temperatures from daily total solar radiation  $S$  is obtained as follows:

$$\Delta T = 0.34S - 1.06 \quad (8)$$

Since the daily solar radiation and daily average ambient temperature can be obtained from JMA database, the internal bearing temperature can be estimated from Eq. (8), and the deterioration of rubber bearing as an effect of solar radiation can be estimated roughly by assuming the internal temperature is uniform in the bearing. By assuming the uniform temperature inside the bearing, the larger aging effect of 10 mm thick region (without 10 mm of the surface rubber) is neglected in this study. It is assumed that the effect will be small when compared to the total effect of solar radiation.

Since the variation of the internal bearing temperature is influenced by some parameters such as thermal properties and geometry of the bearing, and geographical and climatic conditions, Eq. (8) is applicable only for the condition of the experiment of this study. To obtain the equation that can be applied for other conditions, heat transfer analysis to predict the internal temperature of a bearing exposed to solar radiation will be necessary.

#### 4.2 Long-term Performance of HDR Bearing Considering Solar Radiation Effect

Itoh et al.<sup>6)</sup> performed the accelerated thermal oxidation test of HDR blocks and found that there are two factors affecting the aging of HDR: spontaneous reaction and oxidation. The spontaneous reaction occurs in the very early stage of aging and the material properties of the HDR bearing change uniformly in the bearing in a short time. The degree of this spontaneous reaction was found to be dependent on temperature. After the spontaneous reaction reaches a stable state, only the oxidation deterioration continues.

According to the Manual of Highway Bridge Bearing<sup>9)</sup>, the equivalent shear stiffness  $K_h$  of a rubber bearing can be calculated using the following equation:

$$K_h = \frac{GA}{nt_r} \quad (9)$$

where,  $G$  is the static shear modulus of the rubber material,  $A$  is the effective area supporting the superstructure,  $n$  is the number of rubber layers, and  $t_r$  is the thickness of a rubber layer. Due to the heterogeneous aging effect, the static shear modulus varies according to the relative position inside the rubber bearing. Therefore, the equivalent shear stiffness of an aged rubber bearing can be expressed by the following equation:

$$K_h = \frac{\int GdA}{nt_r} = \frac{G_0 \int f(x, y)dA}{nt_r} \quad (10)$$

where,  $G_0$  and  $G$  are the static shear modulus before and after aging, respectively.  $f(x, y)$  is the function expressing the variation of the shear modulus at any position  $(x, y)$  in the

Table 3 Parameters used for aging property estimation

$\alpha$ [ $10^{-4}$ mm]	$\beta$ [ $10^3$ K]	$E_a$ [ $10^4$ J/mol]	R [J/mol/K]	$T_{ref}$ [K]
1.20	3.82	9.04	8.31	333

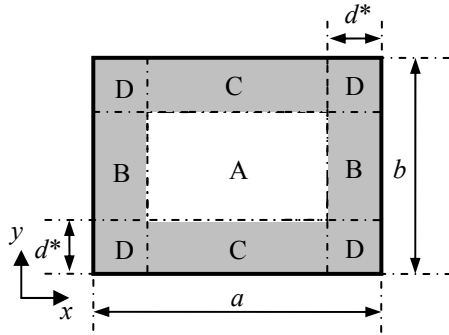


Fig. 20 Cross section of aged rubber bearing

horizontal cross section. Fig. 20 shows the plan of a rectangular rubber bearing is shown with a side length of  $a$  and a width of  $b$ . The critical depth is  $d^*$ , which is a depth beyond which oxidation cannot reach. Critical depth is estimated from Eq. (11)<sup>6</sup>, where the symbols  $\alpha$  and  $\beta$  are constants determined by the thermal oxidation test. The critical depth is determined based on the assumption that bearing temperature is uniform in the cross section.

$$d^* = \alpha \exp\left(\frac{\beta}{T}\right) \quad (11)$$

The variation of the static shear modulus resulting from both the spontaneous reaction and the oxidation can be expressed by the following equations<sup>6</sup>:

$$\Delta f_i = 88.4 \exp\left(\frac{-1887.2}{T}\right) \quad (12)$$

$$\Delta f_s = 9.3 \times 10^{-4} t_{ref} \quad (13)$$

$$\ln\left(\frac{t_{ref}}{t}\right) = \frac{E_a}{R} \left(\frac{1}{T_{ref}} - \frac{1}{T}\right) \quad (14)$$

where,  $E_a$  is the activation energy of HDR,  $R$  is the gaseous constant,  $T$  is the absolute temperature in the service condition,  $T_{ref}$  is the reference temperature used in the accelerated test,  $t$  is the real aging time,  $t_{ref}$  is the equivalent aging time in the accelerated test,  $\Delta f_i$  is a relative change of the static shear modulus due to the spontaneous reaction, and  $\Delta f_s$  is a relative change of the static shear modulus at the surface of the rubber bearing due to oxidation. Eq. (14) translates the aging time under service conditions to the equivalent aging time at the reference temperature in the accelerated aging test using the

Arrhenius methodology. In the research by Itoh et al.<sup>6</sup>, the reference temperature of 60°C was used. The parameters used in this study to estimate the variation of the equivalent shear stiffness are listed in Table 3.

The bearing plan can be divided into four regions, A, B, C and D based on the effect of oxidation as shown in Fig. 20. The effective shear stiffness for each region which considers only oxidation can be calculated as follows<sup>6</sup>,

a. Region A: region beyond the critical depth

The region beyond the critical depth is not influenced by oxidation, and the function  $f(x, y)$  in Region A equals 1. The effective  $GA$  contributed by Region A can be calculated as:

$$(GA)_A = G_0 (a - 2d^*) (b - 2d^*) \quad (15)$$

b. Region B and C: region where one direction of oxidation occurs

Region B is the outer region from the bearing surface to the critical depth in  $x$  direction, while Region C is the outer region in  $y$  direction. The variation of the static shear modulus is assumed to be a quadratic function of the relative position from the surface to the critical depth. For example, in the range  $0 < x < d^*$  of Region B, the function  $f$  is expressed as the following equation:

$$f = f(x) = 1 + w_x \Delta f_s \quad (16)$$

$$w_x = \left(\frac{x - d^*}{d^*}\right)^2 \quad (17)$$

Then the integral of the function  $f$  in each Region B or C is calculated, and the effective  $GA$  of these regions can be written as:

$$(GA)_{B \text{ or } C} = G_0 d^* (a + b - 4d^*) \left(1 + \frac{1}{3} \Delta f_s\right) \quad (18)$$

c. Region D: region where two directions of oxidation occur

In Region D oxygen permeates from two directions, therefore this region is most affected by oxidation. However, when compared to the whole area of the bearing, the area of Region D is relatively small. As a result, the property variation in this region does not affect the overall performance much. The variations of  $f$  in these two directions agree at  $x=y$ . The integral of  $f$  in Region D results in the following equation:

$$(GA)_D = 4G_0 d^{*2} (1 + \Delta f_s / 2) \quad (19)$$

The effective  $GA$  of overall regions after also considering the spontaneous reaction is calculated as follows:

$$GA = \left(\sum_{q=1}^r (GA)_q\right) (1 + \Delta f_i) \quad (20)$$

where  $r$  is the number of regions. In this study, the critical depth and  $\Delta f_i$  are calculated by using the yearly average bearing temperature.

To investigate the long-term performance of HDR bearings

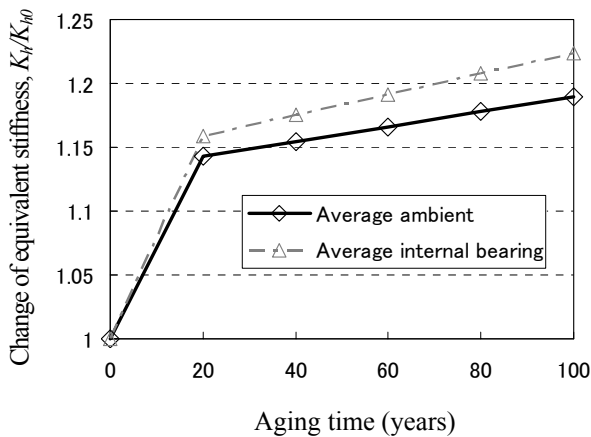


**Fig. 21** Long-term performance of 420 mm x 420 mm HDR bearing in Nagoya

by including solar radiation effects, in this study two kinds of predictions are made:

1. Prediction by using the yearly average ambient temperature.
2. Prediction by using the estimated internal bearing temperature calculated from Eq. (8).

Solar radiation and ambient temperature data of Nagoya from Japan Meteorological Agency in 2004 is used in the prediction. Data in 2004 has the highest value of average ambient temperature within 5 years from 2004 to 2008. The average of ambient temperature in 2004 is 16.8°C. The average of daily total solar radiation in 2004 is 14.3 MJ/m<sup>2</sup>. Eq. (8) gives the average internal bearing temperature of 20.6°C. By using these temperature values, the change of bearing's shear stiffness of an HDR bearing with the size of 420 x 420 mm within 100 years, can be calculated as shown in Fig. 21.

It can be seen in Fig. 21 that the application of the average internal bearing temperature results in the faster change of equivalent shear stiffness. After 100 years aging time, the shear stiffness of HDR bearing increases by 19% when the yearly average ambient temperature is used, while it increases by 22% when the internal bearing temperature by Eq. (8) is used. Except for the bearing exposed to solar radiation, the yearly average ambient temperature can be used to predict the long-term performance of rubber bearing. In Nagoya, the effect of solar radiation on the internal bearing temperature increases the change of bearing equivalent shear stiffness by only 3% of the initial stiffness compared to the one without considering solar radiation. In areas where the solar radiation is large, it may be necessary to evaluate the effect of solar radiation on long-term performance of rubber bearing.

This study proposes the relationship between solar radiation and temperature difference of ambient and internal bearing temperatures based on measurement results. By using daily average solar radiation and daily average ambient temperature

from the JMA database, internal bearing temperature of a certain location can be estimated, and the long-term performance of rubber bearing can be predicted.

## 6. SUMMARY AND CONCLUSIONS

In this study surface temperatures of a bearing installed in an elevated highway in Nagoya, Japan, were measured to evaluate the effect of solar radiation on the bearing temperature. Internal temperature measurement of a bearing model was carried out to understand a temperature variation in a bearing. To accurately predict the long-term performance of rubber bearing exposed to solar radiation, the procedure to consider the solar radiation effect was proposed. The conclusions are summarized as follows:

- 1) Bearing surface temperatures are significantly higher than the ambient temperature when the surface is exposed to solar radiation. The maximum difference from the ambient temperature can be greater than 20°C. When daily average values are compared, the difference between the surface and ambient temperatures is about 4-6°C on a sunny day and about 1-2°C on a rainy day.
- 2) Bearing internal temperature is higher than the ambient temperature in terms of daily averages when the bearing is exposed to solar radiation. For a 420 x 420 mm HDR bearing exposed to solar radiation, the maximum difference is about 7°C.
- 3) Except the bearing exposed to solar radiation, the yearly average ambient temperature can be used to predict the long-term performance of rubber bearing. In Nagoya, the effect of solar radiation on the internal bearing temperature increases the bearing equivalent shear stiffness by 3% of the initial stiffness after 100 years. It is necessary to evaluate the effect for other locations that have large solar radiation to examine the significance of the effect of solar radiation on long-term performance of bridge rubber bearings.

## ACKNOWLEDGMENT:

This research was conducted as part of research projects granted by Nagoya Expressway Public Corporation. The authors wish to express their gratitude to Tokai Rubber Industries, Ltd. for their support to manufacture rubber bearing models.

## References

- 1) Stevenson, A., Longevity of natural rubber in structural bearings, *Plastics and Rubber Processing and Applications*, Vol.5, p.253-258, 1985.
- 2) Derham, C.J., Thomas, A.G. and Kelly, J.M., A rubber bearing system for seismic protection of structures, *Proceedings of Conference on Engineering Design for Earthquake Environments*, pp.53-58, 1978.
- 3) Watanabe, Y., Kato, A., Yoneda, G., and Hirofani, T.,

- Ageing effects of forty years old laminated rubber bearings, *Proceedings of the 1<sup>st</sup> Isolation and Structural Control Design Colloquium*, pp.439-446, 1996.
- 4) Itoh, Y., Satoh, K., Gu, H. S., and Yamamoto, Y., Study on the long-term deterioration of natural rubber of bridge bearings, *Journal of Structural Mechanics and Earthquake Engineering*, JSCE, No.801/I-73, pp.185-196, 2005 (in Japanese).
  - 5) Itoh, Y., Satoh, K., Gu, H. S., and Yamamoto, Y., Study on the deterioration characteristics of natural rubber bearings, *Journal of Structural Mechanics and Earthquake Engineering*, JSCE, Vol.62, No.2, 2006 (in Japanese).
  - 6) Itoh, Y., Gu, H. S., Satoh, K., and Yamamoto, Y., Long-term deterioration of high damping rubber bridge bearing, *Journal of Structural Mechanics and Earthquake Engineering*, JSCE, Vol.62, No.3, pp.595-607, 2006.
  - 7) Itoh, Y., and Gu, H. S., Predictions of Aging Characteristics in Natural Rubber Bearing Used in Bridges, *Journal of Bridge Engineering*, ASCE, Vol.14 No. 2, pp. 122-128, 2009.
  - 8) Matsuda, T., Nishi, T., Sudoh, C., and Yazaki, F., Validity evaluation and ISO standardization of property prediction technology based on actual measurement of isolators used for 10 years, *Proceedings of Annual Conference of the Japan Society of Civil Engineers*, Vol. 58, pp. 765-766, 2003 (in Japanese).
  - 9) Itoh, Y. and Gu, H. S., Effect of ultraviolet irradiation on surface rubber used in bridge bearing, *Journal of Structural Engineering*, JSCE, Vol.53A, pp. 696-705, 2007.
  - 10) Japan Road Association, *Design Specifications of Highway Bridges V*, 2002 (in Japanese).
  - 11) JRA, *Manual of Highway Bridge Bearing*, 2004 (in Japanese).
  - 12) Gu, H. S. and Itoh, Y., Seismic response of steel bridge piers with aged base-isolated rubber bearing, *Journal of Structural Engineering*, JSCE, Vol.52A, pp.537-546, 2006.
- (Received September 24, 2009)